J. Biochem. **95**, 213-221 (1984)

Topographic Analysis of the Redox State of Rat Brain by NADH Fluorescence Photography of Cross Sections[1]

Toshihisa ISHIKAWA,* Mamoru TAMURA,* Shizuo NAKAMURA,** Mitsuho IKEDA,*** and Katsuya NAGAI***

*Biophysics Division, Research Institute of Applied Electricity, Hokkaido University, Sapporo, Hokkaido 060, **Sensory Informatic Engineering Division, Research Institute of Applied Electricity, Hokkaido University, Sapporo, Hokkaido 060, and ***Division of Protein Metabolism, Institute of Protein Research, Osaka University, Suita, Osaka 565

Received for publication, June 28, 1983

Two-dimensional changes of the redox level of NADH were measured by fluorescence photography with the aid of computer-processing in cross sections of rat brain that had been frozen *in situ* in liquid nitrogen. Structure-related heterogeneity was noted in the distribution of the redox level in normal brain of conscious rats. Using 2-deoxy-[^{14}C]glucose autoradiography, the area showing relatively high NADH fluorescence was found to be the area of high glucose utilization. Quantitatively, however, the fluorescence intensity did not parallel the rate of glucose uptake.

Increase of NADH fluorescence was observed specifically in the nucleus caudatus putamen and the thalamus when the rats were anesthetized with pentobarbital. Chemical determination of the NADH content was also performed simultaneously, and the results were consistent with those obtained by fluorescence photography.

Because of the functional heterogeneity of the brain, space-dependent measurements are crucial in determining the correlation of energy metabolism with functional neural activity. The 2-dexoy-[^{14}C]glucose method (*1*) has been most widely used for this purpose. The area showing a higher glucose uptake is the area where energy metabolism is active, in other words, where nervous functional activity is high. The topographic representatior technique for measurement of ATP (*2*) and pH (*3*) have also been developed. A link between metabolism and function was suggested earlier through the concept of respiratory control demonstrated in isolated mitochondria by Lardy and Wellman (*4*) and Chance and Williams (*5*). The correlation of the redox state with electrical activity of the brain was investigated by Mayevsky *et al.* by monitoring the fluorescence of the brain surface of unanesthetized rats (*6*). The method of NADH fluorescence photography was developed by Chance and coworkers (*7*, *8*). This method clearly demonstrated two-dimensional changes of redox level in the cerebral cortex. Welsh *et al.* applied this technique to cross sections of frozen brain to determine the effect of ischemia on regional metabolic changes (*9-11*).

[1] This study was supported by a Grant-in-Aid for Scientific Research (57440097) from the Ministry of Education, Science and Culture of Japan.

Here we used NADH fluorescence photography of cross sections of freeze-trapped rat brain to map the redox state of brain tissues, and also examined the redox level of NADH quantitatively by processing fluorescence photographs with a computer. Results were also compared with those on the NADH content determined by chemical assay.

EXPERIMENTAL PROCEDURES

Fluorescence Photograph of NADH in Rat Brain—Male Wistar strain rats (body weight, 280–360 g) were used and fluorescence photography was performed by Welsh's method (*9–11*) with slight modifications. In brief, brains from rats in various conditions (conscious normoxic, ischemic and anesthetized) were frozen *in situ* in liquid nitrogen. The brain was sectioned at 100 μm intervals with a microtome in the coronal plane at -20°C on a cryostat stage. Figure 1 shows a block diagram of the apparatus for fluorescence measurement. The cross sectional surface of the frozen brain was illuminated uniformally with UV light centered at 360 nm from a 150 W Xenon lamp through a quartz light guide of 1 cm diameter. Emission from the section was recorded on Kodak recording film 2475 with a 35 mm camera (Minolta SR-1) through a filter placed on the lens. A Corning filter No. 5840 and a combination of Hoya B 460 and Y44 filters were used for excitation and emission measurements, respectively. The optical characteristics of these filters are given in Fig. 3.

The fluorescence photograph required 30 s exposure at an aperture of f/5.6. For comparison of photographs obtained with different brain preparations, a small frozen quartz vessel containing the same concentration of NADH (1–3 μM) was placed on the cryostat stage near the brain section, and photographed with the section. The fluorescence intensity of the frozen NADH solution in the photograph was used as an internal standard. The linearity of the intensity of NADH fluorescence was calibrated from photographs of the frozen standard NADH solution. A reflection photograph at 360 nm, obtained without the filter attached to the camera (Filter 2) of the same cross section was also taken to check hemodynamic changes.

Optical Density Measurement of Negative Film and Computer Processed Three-Dimensional Representation—In the photographic process, the intensity of the light, the number of photons, is converted to the density in the developed negative film, which is a function of the exposure, product of incident light energy flux times duration. Here, there is the condition that the light intensity is equivalent to the duration. Under the suitable conditions which we employed, the density was

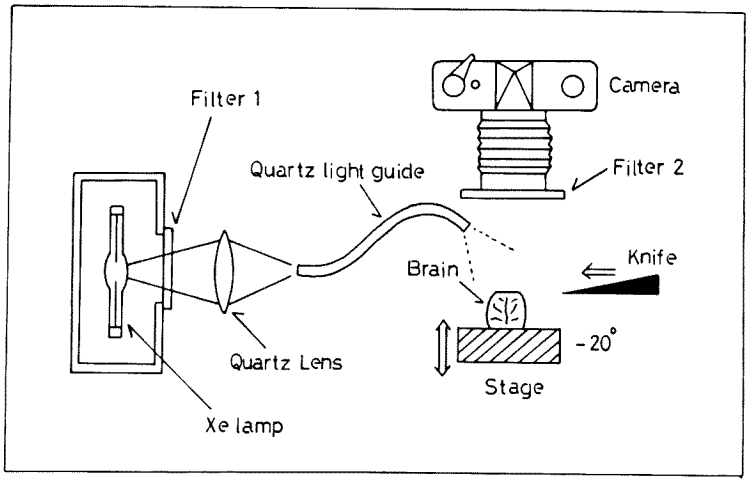

Fig. 1. Schematic illustration of the apparatus for NADH fluorescence photography. Filters 1 and 2 are for excitation and emission, respectively, and their optical characteristics are given in Fig. 3.

linearly related to the logarithm of the exposure. Thus, the photograph is a logarithmic recording apparatus for the intensity of the light.

The density of the negative film was converted to the "optical density" by taking the logarithm of the ratio of the incident and transmitted lights through the film. For three-dimensional representation, the optical density of each point in the negative film was measured and digitized with a DEC PDP-11 23L computer which controlled drum scan flying spot densitometer coupled with an A/D converter (Fig. 2). The digital data were stored on a floppy disc and then processed with the same computer system. Initially 512 × 512 data points were digitized by 8-bit and the mean value of each point was calculated by the area-mean method. The resultant grey levels of each point were converted to continuous lines. After smoothing the lines, an appropriate interval of the lines was chosen by picking up. The curves were plotted as three-dimensional representations, where the fluorescence intensity at each point was converted to height, after normalization and Euler-angle-transformation. Details of digital image processing are given in Ref. *12*. When necessary, the cross section at any optional axes could be given (*cf.* Fig. 8). The program of the system was registered in the User-Files of Hokkaido University.

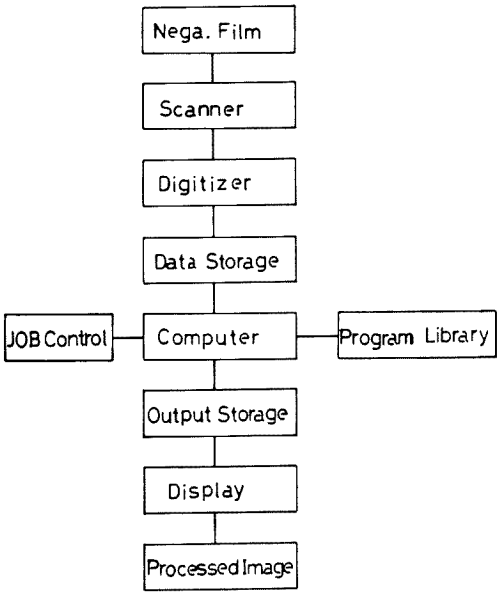

Fig. 2. Block diagram for three-dimensional representation of NADH photographs.

Fluorescence Spectra of Rat Brain—The fluorescence spectra of rat brain were measured in a Hitachi fluorometer, model MPF4. The cross section of the frozen brain was placed at 45° to the excitation light, and emitted light was measured. The excitation spectra of the brain were measured similarly. The excitation beam was more than 5 mm in diameter and therefore, the resultant fluorescence spectra were means for various areas of the cross section.

[^{14}C]2-Deoxyglucose Autoradiography—The rate of glucose uptake was measured by the 2-deoxy-[^{14}C]glucose method (*1*). 2-Deoxy-[^{14}C]-glucose (150 μCi/kg) was injected into the right atrium of the heart through a catheter. One hour later, rats were killed and physiological saline was promptly infused into the carotid artery to remove blood from the brain. Then the brain was frozen in liquid nitrogen and sectioned at 100 μm thickness, and the slices were exposed to LKB 2208 Biofilm for 15 days.

Biochemical Determination—For determination of regional concentrations of NADH, brain tissue of 1.5 mm diameter and 1.0 mm depth was taken from sections of frozen brain. Tissue samples were suspended in 100 μl of 0.1 N NaOH in methanol at −20°C and then homogenized at 4°C in 2 ml of 0.01 N NaOH solution. The homogenate was mixed with 1 mM cysteine, heated for 10 min to destroy NAD^+, and then neutralized with perchloric acid. Its NADH content was measured by the enzymatic cycling method of Kato *et al.* (*13*) in an ATP meter (Analytical Luminescence Laboratory Co., Ltd.).

Materials—Alcohol dehydrogenase [EC 1.1.1.1] from yeast, glutamic oxaloacetic transaminase [EC 2.6.1.1] from pig heart, malate dehydrogenase [EC 1.1.1.37], and NADH were purchased from Boehringer Mannheim. Other chemicals used were analytical grade products obtained from local sources.

RESULTS

Fluorescence Characteristics of Freeze-Trapped Rat Brain—Figure 3 shows fluorescence excitation and emission spectra of a cross section of rat brain at −20°C. Excitation light at 340, 360, and 380 nm gave almost identical emission spectra with a maximum at 457 nm, though their relative

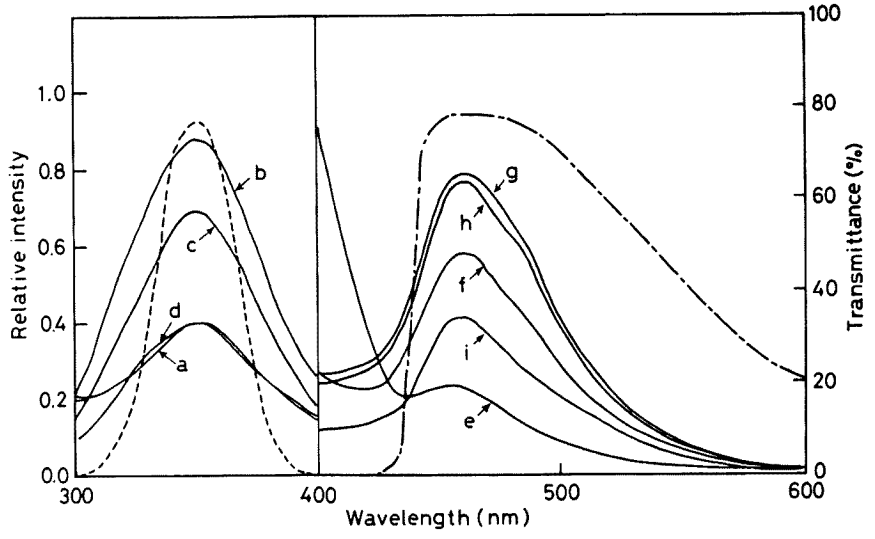

Fig. 3. Fluorescence spectra recorded from the surface of a cross section of frozen brain and optical characteristics of the filters used for fluorescence photography. ----, transmittance of the filter for excitation; -----, transmittance of the filter for emission measurement. The brain was frozen in liquid nitrogen 5 min after decapitation. Fluorescence was measured on the cross section 6 mm anterior to the external auditory meatus. The cross section was kept at −20°C during the measurement. Excitation spectra of emission were measured at 440 (a), 465 (b), 480 (c), and 500 nm (d). Emission spectra were excited at 300 (e), 320 (f), 340 (g), 360 (h), and 380 nm (i).

intensities differed. Spectra excited at 300 nm had strong emission at wavelengths below 400 nm, the source of which has not yet been identified. When illuminated with light at 300 nm, the white matter showed this emission. The excitation spectra measured at emission wavelengths of 465, 480, and 500 nm were almost identical, with a maximum at 340 nm. The spectrum with excitation at 440 nm differed slightly from other spectra at wavelengths shorter than 320 nm. The over-all patterns of both emission and excitation spectra resembled those of reduced pyridine nucleotide. The emission maximum of the spectra from brain were shifted approximately 10 nm to longer wavelengths than that of NADH solution, as observed in other tissues and mitochondria (*14*). Thus, we used optical filters with the characteristics shown in Fig. 3 for photography of fluorescence of reduced pyridine nucleotide. The fluorescence was mainly that of NADH, since the NADH content is more than 5-times that of NADPH in the brain (*15*).

Normoxic Conscious Rat Brain—Figure 4A shows a typical fluorescence photograph obtained from the brain of a normal conscious rat. A schematic illustration of the cross section is presented in Fig. 4C. In the photograph, the bright area is the region with high NADH fluorescence. The fluorescence intensity was higher in the grey matter than in the white matter. The area around the commissura fornicis ventralis or ventral fornical commissure had very low fluorescence intensity whereas that of the cortex, nucleus caudatus putamen, and nucleus anterior hypothalami had high fluorescence. The NADH contents of cerebral cortex, nucleus caudatus putamen, globus pallidus, and nucleus anterior hypotalami were 13 ± 2, 17 ± 2, 8 ± 1.6, 20 ± 4 nmol/g wet wt, respectively, and were proportional to the fluorescence intensity of the photographs (*cf.* Fig. 6). Figure 4B shows a 2-deoxy-[^{14}C]glucose autoradiograph of an identical section to that of Fig. 4A, where the dark area shows the region with a higher rate of glucose uptake. The rates of glucose uptake were high in cerebral cortex, nucleus caudatus putamen, and nucleus paratenialis, and low in globus pallidus, truncus corporis callosi, nucleus anterior hypothalami, and commisura fornics

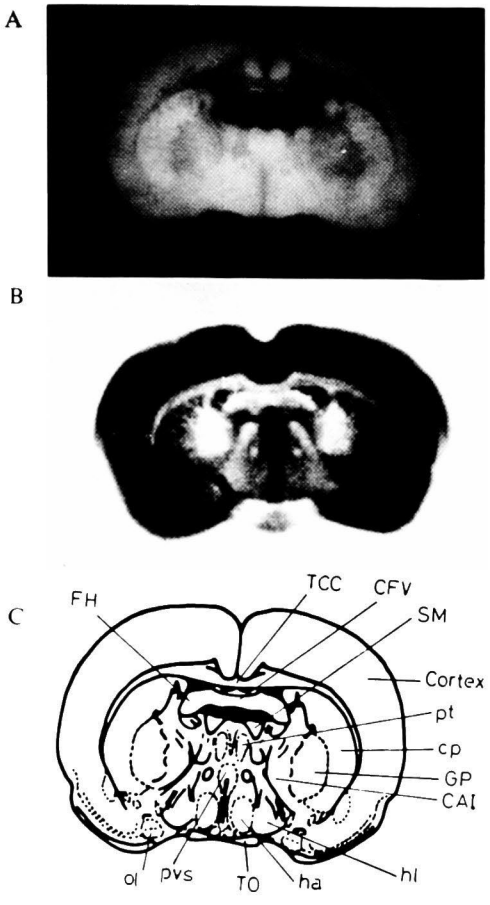

Fig. 4. Fluorescence photograph of a cross section of rat brain. A: The brain of a normal conscious rat was frozen *in situ* in liquid nitrogen. The cross-sectional surface corresponds to a place about 6 mm anterior to the level of the external auditory meatus. B: 2-Deoxy-[^{14}C]glucose autoradiograph of the brain. C: Map of the cross section surfaces corresponding to A and B, cited from Konig and Klippel (*17*). Abbreviations: TCC, truncus corporis callosi; CFV, commissura fornicis ventralis; SM, stria medullaris thalami; pt, nucleus paratenialis; cp, nuclelus caudatus putamen; GP, globus pallidus; hl, nucleus lateralis hypothalami; ha, nucleus anterior hypothalami; pvs, nucleus priventricularis stellatocellularis; ol, nucleus tractus olgactori lateralis; CAI, capsula interna; FH, fimbria hippocampi; TO, tractus optics.

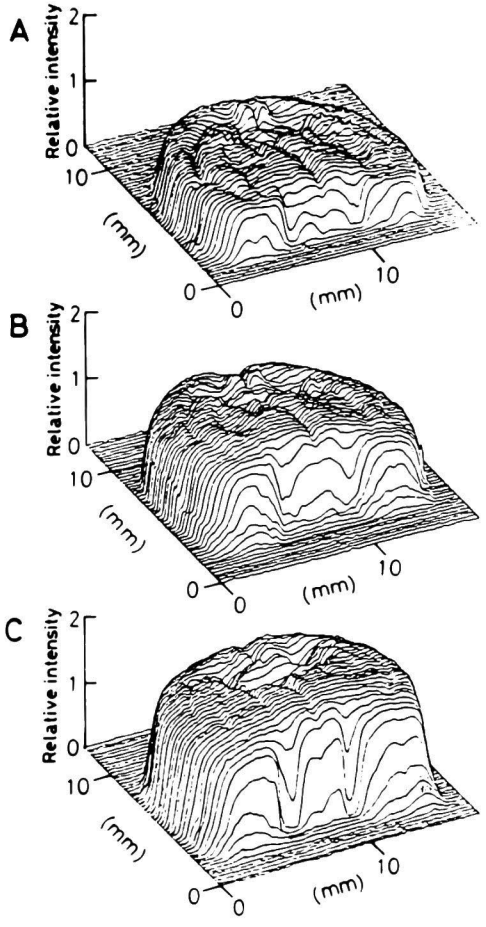

Fig. 5. Three-dimensional representation of fluorescence intensity of rat brain in conscious normoxia and ischemia. The cross section is identical in position to that in Fig. 4. A: Normoxia. The three-dimensional representation was obtained by processing the fluorescence photograph of Fig. 4A. B: 20 s after decapitation. C: 5 min after decapitation.

ventralis. The absolute values of glucose uptake of those area are given in Table II. Thus, the distributions of glucose uptake and NADH fluorescence intensity were not identical to each other.

Normoxic-Anoxic Transition—Figure 5 shows a topographic representation of fluorescence photographs of brain sections in normoxia (A) and ischemia (B and C). The representation in conscious normoxia obtained from the photograph of Fig. 4A expresses the distribution of fluorescence intensity as peaks and valleys. The cortex and nucleus caudatus putamen gave a mountain range and tableland, respectively. The heterogeneity observed in normoxia faded away during development of ischemia (Fig. 5, B and C). In complete ischemia (Fig. 5C; 5 min after decapitation) the height was about twice that in normoxia, and the distribution of fluorescence intensity became almost uniform over the cross section.

Figure 6 shows the regional changes in NADH content induced by ischemia. In normoxia, the NADH content of the globus pallidus was slightly lower than those of the cortex, nucleus caudatus putamen, and nucleus anterior hypothalami. The results are consistent with those of the fluorescence photograph (Fig. 4A). In complete ischemia, occurring 5 min after decapitation, the NADH contents of all areas were 5 to 6 times those in normoxia, and so differences between brain areas were not statistically significant, as seen from the fluorescence photographic data (Fig. 5C). The NADH contents 20 s after decapitation were intermediate between those of normoxia and complete ischemia (5 min) except in the nucleus anterior hypothalami. The higher NADH content in this area observed 20 s after decapitation could not be attributed to delay in the freezing front, since the NADH content in normoxia was similar to that of other areas such as the nucleus caudatus putamen. The time course of the apparent optical density change in the photograph (Fig. 7) was similar to that found on chemical assay of NADH. The time course of lactate accumulation was also similar to that in Fig. 7 (*16*).

Pentobarbital-Anesthetized Rat Brain—Differences in NADH in specific areas were also observed in the brain of rats anesthetized with pentobarbital, as shown in Fig. 8. Figure 8A is a fluorescence photograph of a brain section in normoxia, which is a nearly identical section to that in Fig. 4A. Figure 8B shows the three-dimensional representation of Fig. 8A. The distribution of fluorescence intensity along the X-Y line in Fig. 8A is given in Fig. 8C, where the distributions of normoxic and anoxic conscious rat brains were also superimposed in the figure. The fluorescence is increased specifically in the nucleus caudatus putamen, and the extent of increase over that in normoxia is about 30% of the increase observed in complete ischemia. Anesthesia also caused about 20% increase in fluorescence in the thalamus, which lies posterior to this section (data not shown). The reflection photograph without Filter 2 shown in Fig. 1 of the anesthetized rat brain was identical to that of conscious normoxic rat brain. Thus, the changes in NADH fluorescence were not due to a hemodynamic artifact.

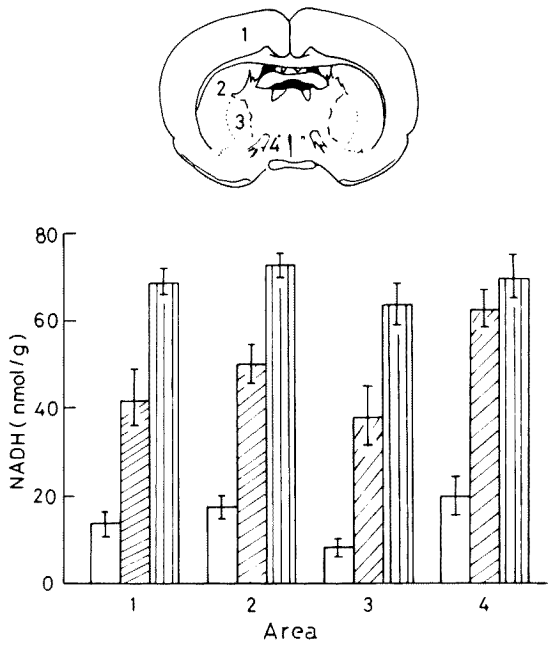

Fig. 6. Regional NADH concentration in normoxic and ischemic brain. Brains were frozen in liquid nitrogen *in situ* in normoxia or 20 s and 5 min after decapitation. In each case, samples from 5 animals were measured. The error brackets indicate S.E. The areas measured are shown at the top. Areas: 1, cerebral cortex; 2, nucleus caudatus putamen; 3, globus pallidus; 4, nucleus anterior hypothalami. ☐, conscious normoxia; ▨, 20 s after decapitation; ▥, 5 min after decapitation.

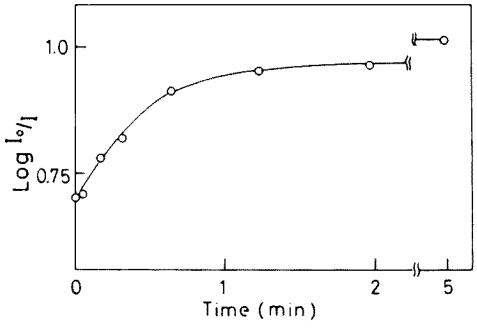

Fig. 7. Time course of change in optical density in NADH fluorescence photographs induced by ischemia. Brain was frozen at appropriate intervals after decapitation. Photographs were taken from the corresponding cross section. Each circle represents the value obtained in a different rat brain. Films were placed in the cell compartment of the spectrophotometer at right angles to the light beam and apparent optical density (log I_0/I), was recorded. Optical density was the mean for the cortex and nucleus caudatus putamen. I, transmitted light; I_0, incident light.

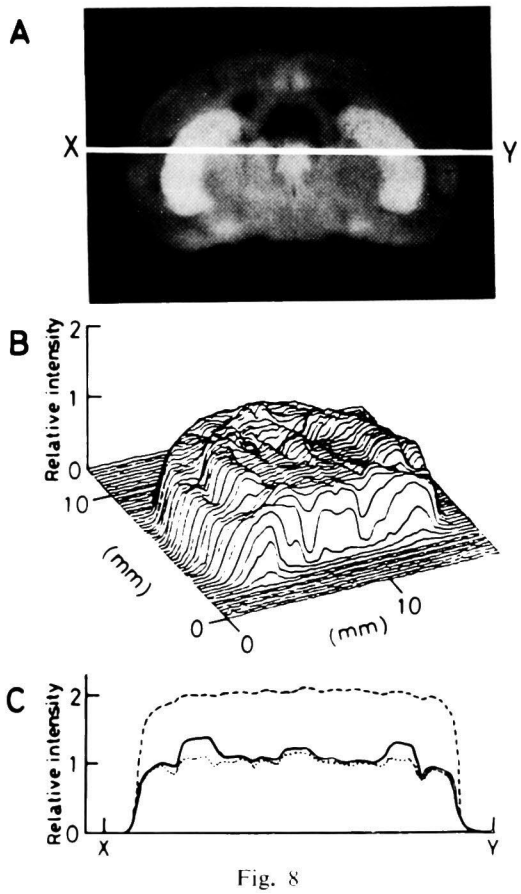

Fig. 8

The NADH contents in cerebral cortex, nuclues caudatus putamen, and nucleus anterior hypothalami were compared between anesthetized and non-anesthetized rats (Table I). The rate of glucose uptake was also given in Table II. As can be seen, the NADH content of the nucleus caudatus putamen was about 1.4 times that of unanesthetized rat brain. There was no significant difference between the NADH contents of the cerebral cortex or nucleus anterior hypothalami of anesthetized and conscious rats. Table II shows the effect of pentobarbital anesthesia on local cerebral glucose uptake in rat brain. By anesthesia, the glucose uptake in cortex (olfactory, somato-sensory) and nucleus caudatus putamen

Fig. 8. Effect of pentobarbital anesthesia on the distribution of NADH fluorescence intensity. The rat was anesthetized by intraperitoneal injection of pentobarbital (40 mg/kg body weight), and 20 min later it was decapitated and its brain was frozen. A: Fluorescence photograph of anesthetized rat brain. B: Three-dimensional representation of the fluorescence intensity of A. C: Distribution of fluorescence intensity along the line X-Y in A, (——). The distributions in conscious normoxic brain (·····) and completely ischemic brain (----) were obtained along identical lines to the X-Y line in Fig. 5A.

TABLE I. Regional NADH content in brain of pentobarbital anesthetized rats. Values are given in nmol/g and mean ± S.E. The data were the mean of 5 and 3 rats for control and pentobarbital anesthesia, respectively.

	Control	Anesthetized
Cerebral cortex	13.3 ± 1.6	13.9 ± 1.1
Nucleus caudatus putamen	17.3 ± 1.3	23.4 ± 1.2
Globus pallidus	19.7 ± 1.9	19.8 ± 1.2

TABLE II. Effect of pentobarbital anesthesia on local glucose utilization. Values are μmol/100 g·min and mean ± S.E. The number in parentheses indicates the number of experiments. Pentobarbital (40 mg/kg·body weight) was administered 10 min before [^{3}H]deoxyglucose injection.

	Control (4)	Anesthesia (5)
Cerebral cortex		
Frontal cortex	122 ± 9	66 ± 4
Somato-sensory cortex	111 ± 5	60 ± 5
Auditory cortex	122 ± 14	69 ± 6
Visual cortex	104 ± 12	61 ± 4
Thalamus		
Lateral nucleus	98 ± 8	60 ± 6
Ventral nucleus	80 ± 7	54 ± 6
Caudatus putamen	102 ± 8	54 ± 5
Globus pallidus	53 ± 4	42 ± 5
Hypothalamus	82 ± 10	57 ± 7
Hippocampus	82 ± 8	59 ± 7
Corpus callosum	33 ± 7	30 ± 7

were decreased to about half of those in conscious rat. In contrast, those in globus pallidus, hypothalamus, and thalamus decreased 20–30%. For comparison, white matter (corpus collosum) changed little.

DISCUSSION

As seen in Figs. 4 and 5, NADH fluorescence in normal conscious rat brain has a very heterogeneous distribution. This heterogeneous distribution probably reflects that of the redox level of NADH/NAD, rather than that of the NADH content of brain structures, since in complete ischemia cross sections of the brain showed a uniform distribution of fluorescence of high intensity. In conscious normoxic brain, the redox level of NADH/NAD tends to shift toward reduction in the gray matter where glucose uptake is relatively high (*cf.* Figs. 8, 4, and Table II). However, quantitatively there was no parallelism between the redox state of NADH/NAD and glucose uptake. For example, the globus pallidus showed almost the same fluorescence intensity as cerebral cortex, but glucose uptake in this area was very low (*cf.* glucose uptakes for cerebral cortex and globus pallidus were 110 ± 5 and 53 ± 4 μmol/100 g min wet wt. respectively). A similar phenomenon was observed in the nucleus anterior hypothalami. In contrast, capsula interna and commisura fornicis ventralis showed similar glucose uptake, but the fluorescence intensity of the latter was low (~70% of the former). The non-parallelism was also observed in the brain of anesthetized rat.

It is remarkable, but puzzling, that on pentobarbital anesthesia in normoxia fluorescence increase occurred specifically in the nucleus caudatus putamen and thalamus, because the former is concerned with associated movements and the latter with sensation. The possibility of anoxia due to decrease in cerebral blood flow is inconsistent with the finding of Siesjo *et al.* (*18*, *19*) that the ATP and creatine phosphate concentrations in the brain did not decrease in anesthesia. An alternative explanation is as follows: During state 3-state 4 transition of mitochondria, the respiration rate decreases, with a shift of the redox state of NADH/NAD towards reduction under aerobic conditions (*5*, *20*). Based on this idea, the results in Fig. 5 may be related to decrease in the respiration rate in these structures due to decreased nervous functional activity. Indeed, the glucose uptake in caudatus putamen and thalamus of anesthetized rat brain were about half of that of conscious rat (Table II). Globus pallidus showed a slight decrease in glucose utilization due to anesthesia, concomitant with little change of NADH fluorescence. Instead, it is also noted that though glucose uptake in cerebral cortex was decreased by anesthesia to about half of that of conscious rat, NADH fluorescence changed little (Table II and Fig. 8).

The tissue NADH/NAD ratio is regulated by several factors such as intracellular oxygen concentration, respiratory rate, and glycolytic flux (*20–22*). The energy state of the tissue, phosphate potential (ATP/ADP P_i), is also the major determinant for the redox state (*22*). Thus, the factors determining the redox level of NADH/NAD differ in different areas, and therefore the mechanism of NADH reduction in Fig. 8 may differ from that in normal conditions, especially in cerebral cortex in Fig. 4.

Results on the NADH content measured by chemical assay were consistent with the results of fluorescence measurements (Fig. 6 and Table I). The values in Fig. 6 were slightly higher (~20%) than those determined by microwave irradiation (*15*). This difference may be due to a difference in fixation methods. In our method, 10–15 s was required for the central area of the brain to reach 0°C. Quantitatively, however, the changes in fluorescence intensity were smaller than the changes in NADH content measured by chemical assay. For example, the NADH content in complete ischemia was more than 4-fold that in normoxia (Fig. 6), whereas the fluorescence intensity increased only about 2-fold in the same conditions. The results in Fig. 7 and Table I show similar phenomena. This difference may be explained as follows. First, fluorescence measurement reflects mainly the redox level of NADH/NAD in mitochondria rather than in the cytosol (*10*, *14*), whereas the chemical assay measures the NADH content in both. Second, there is a non-specific background fluorescence in tissue excited with UV-light (*cf.* Fig. 3) (*10*). Third, the negative film has non-linear sensitivity (logarithmic), which depends on the conditions of exposure and development. This non-linearity can be overcome

by using an internal standard.

As the redox level of NADH/NAD is a complex function of the tissue metabolism, simultaneous measurement by computer-assisted NADH fluorescence photography and autoradiography of 2-deoxy-[^{14}C]glucose will provide quantitative information about the energy state and regulation of energy metabolism in relation to neural activity in the brain. However, there are some difficulties upon processing the autoradiography. Exposure requires an extremely long period (usually a month), where we must test the linearity between the density and absolute counts. Autoradiograms show very rough distribution in the density, which generates large noise during the optical scanning. Thus, we must employ a different type of processing than that used for the fluorescence photographs. The details of the three-dimensional analysis of the autoradiographs of 2-deoxy[^{14}C]-glucose and [^{14}C]antipyrine will be given in the near future; the latter is the indicator for local blood flow (*23*). The method employed here could be used for mapping the redox states of various cytochromes by taking reflectance photographs under illumination with monochromatic light at a specific wavelength for the cytochrome. A highly sensitive TV-camera combined with computer-assisted image processing is now commercially available, and could be used to follow three-dimensional metabolic changes occurring *in situ*.

We thank Dr. N. Oshino, Profs. H. Nakagawa and I. Yamazaki for their encouragement and discussion given during the course of the investigation.

REFERENCES

1. Sokoloff, L., Reivich, M., Kennedy, C., Des Rosiers, M.H., Patlak, C.S., Pettigrew, K.D., Sakurada, O., & Shinohara, M. (1977) *J. Neurochem.* **28**, 897–916
2. Kogure, K. & Alonso, O.F. (1975) *Brain Res.* **154**, 273–284
3. Kogure, K., Alonso, O.F., & Martinez, E. (1980) *Brain Res.* **195**, 95–109
4. Lardy, H.A. & Wellman, H. (1952) *J. Biol. Chem.* **195**, 215–224
5. Chance, B. & Williams, G.R. (1955) *J. Biol. Chem.* **217**, 409–427
6. Mayevsky, A., Jamieson, D., & Chance, B. (1974) *Brain Res.* **76**, 481–491
7. Stuart, B.H. & Chance, B. (1974) *Brain Res.* **76**, 473–479
8. Ji, S., Chance, B., Stuart, B.H., & Nathan, R. (1977) *Brain Res.* **119**, 357–373
9. Welsh, F.A., Durity, F., & Langfitt, T.W. (1977) *J. Neurochem.* **28**, 71–79
10. Welsh, F.A. & Rieder, W. (1978) *J. Neurochem.* **37**, 299–309
11. Welsh, F.A., O'Connor, M.J., & Mancy, V.R. (1978) *J. Neurochem.* **31**, 311–319
12. Castremen, K.R. (1979) *Digital Image Processing* Prentice-Hall Inc., New Jersey, U.S.A.
13. Kato, T., Berger, S.J., Carter, J.A., & Lowry, O.H. (1973) *Anal. Biochem.* **53**, 86–97
14. Chance, B., Williamson, J.R., Jamieson, D., & Schoener, B. (1965) *Biochem. Z.* **341**, 357–377
15. Medina, M.A., Deam, A.D., & Stabinoha, W.B. (1980) in *Cerebral Metabolism and Neural Function* (Passonneau, J.V., Hawkins, R.A., Lust, W.D., & Welsh, F.A., eds.) pp. 56–69, Williams and Wilkins, Baltimore
16. Lowry, O.H., Passonneau, J.V., Hasselberger, F.X., & Schulz, D.W. (1964) *J. Biol. Chem.* **239**, 18–30
17. Konig, J.F.R. & Klippel, R.A. *The Rat Brain* Robert E. Krieger Publishing Co., Inc., Baltimore
18. MacMillan, V. & Siesjo, B.K. (1973) *J. Neurochem.* **20**, 1669–1681
19. Nilsson, L. & Siesjo, B.K. (1974) *J. Neurochem.* **23**, 29–36
20. Sugano, T., Oshino, N., & Chance, B. (1974) *Biochem. Biophys. Acta* **347**, 340–358
21. Bucher, T., Brauer, B., Conza, A., Klein, F., Langguth, O., & Sies, H. (1972) *Eur. J. Biochem.* **27**, 301–317
22. Wilson, D.F., Owen, C.S., & Holian, A. (1977) *Arch. Biochem. Biophys.* **182**, 749–762
23. Tamura, M., Ishikawa, T., Nakamura, S., & Oshino, N. *J. Biochem.* in press